A 700 GHz unilateral finline SIS mixer fed by a multi-flare angle smooth-walled horn

Boon-Kok Tan[a], Ghassan Yassin[a], Paul Grimes[a], Jamie Leech[a],
Karl Jacobs[b], Stafford Withington[c], Mike Tacon[a] and Christopher Groppi[d]

[a]Dept. of Physics (Astrophysics), University of Oxford, Keble Road, Oxford, OX1 3RH, UK.
[b]KOSMA, I. Physikalisches Institut, University of Cologne, Germany.
[c]Cavendish Laboratory, JJ Thomson Avenue, Cambridge CB3 0HE, UK.
[d]ASU School of Earth and Space Exploration PO Box 871404 Tempe, AZ 85287-1404

ABSTRACT

We present the design of a broadband superconductor-insulator-superconductor (SIS) mixer operating near 700 GHz. A key feature of our design is the utilisation of a new type of waveguide to planar circuit transition comprising a unilateral finline taper. This transition is markedly easier to design, simulate and fabricate than the antipodal finline we employed previously. The finline taper and the superconducting circuitry are deposited on a 15 μm thick silicon substrate. The employment of the very thin substrate, achieved using Silicon-On-Insulator (SOI) technology, makes it easy to match the incoming signal to the loaded waveguide. The lightweight mixer chip is held in the E-plane of the waveguide using gold beam leads, avoiding the need for deep grooves in the waveguide wall. This new design yields a significantly shorter chip, free of serrations and a wider RF bandwidth. Since tuning and all other circuits are integrated on the mixer chip, the mixer block is extremely simple, comprising a feed horn and a waveguide section without any complicated mechanical features. We employ a new type of smooth-walled horn which exhibits excellent beam circularity and low cross polarisation, comparable to the conventional corrugated horn, and yet is easier to fabricate. The horn is machined by standard milling with a drill tool shaped into the horn profile. In this paper, we describe the detailed design of the mixer chip including electromagnetic simulations, and the mixer performance obtained with SuperMix simulations. We also present the preliminary measurements of the smooth-walled horn radiation patterns near the mixer operating frequencies.

Keywords: Superconductor-Insulator-Superconductor mixer, unilateral finline taper, Silicon-On-Insulator technology, smooth-walled horn, direct-drilling technique.

1. INTRODUCTION

A major aim of designing a heterodyne detection system for submillimetre wave astronomical observation is to construct a simple yet cost-efficient multi-pixel compact array receiver. The largest heterodyne imaging array constructed to date is the 64-pixel SuperCam spectrometer designed to operate at 870 μm.[1] This is to be compared with the bolometric arrays at submillimetre wavelength such as SCUBA-2[2] that has over 10,000 pixels, which is an order of magnitude larger than SuperCam. To achieve the above-mentioned goal, we present two key improvements to the conventional heterodyne detector design. First, we use a unilateral finline-tapered mixer and second, we use a multi-flared angle smooth-walled horn to replace the conventional corrugated horn.

A major advantage of a finline mixer is that the RF propagation path is oriented along the axial axis of the feedhorn. The entire mixer chip is housed within the waveguide located at the back of the feedhorn. No complicated waveguide structure such as backshort or E-plane tuner is required. The large chip substrate allows the mixer circuitry to be integrated elegantly on a single substrate using planar circuit technology. This simplifies the closed-packed imaging array design. The lateral area occupied by a single mixer unit is completely defined by the footprint of the feedhorn aperture.

Further author information: (Send correspondence to Boon-Kok Tan.)
B-K. Tan: E-mail: tanbk@astro.ox.ac.uk, Telephone: +44 (0) 1865 273303
G. Yassin: E-mail: g.yassin1@physics.ox.ac.uk, Telephone: +44 (0)1865 273440

Millimeter, Submillimeter, and Far-Infrared Detectors and Instrumentation for Astronomy V,
edited by Wayne S. Holland, Jonas Zmuidzinas, Proc. of SPIE Vol. 7741, 774110
 · doi: 10.1117/12.856711

(a) Antipodal finline structure (b) Unilateral finline structure

Figure 1. Two different type of finline taper. The diagram is not drawn to the actual dimensional ratio.

Finline mixers use either antipodal or unilateral fins to couple RF signal from the waveguide to the SIS junction. As shown in Figure 1, antipodal finline structure transform the electromagnetic wave from a waveguide mode to a microstrip mode, whereas a unilateral finline structure converts it to a slotline mode. Antipodal finline mixers have been fabricated and tested rigorously by Yassin et. el.[3–5] These mixers demonstrate performance comparable to the conventional waveguide-probe mixers.

One shortcoming of an antipodal finline taper is that the overlapping fins are susceptible to shorting during the fabrication process. The electromagnetic behaviour of an antipodal finline mixer is also hard to simulate. Unilateral finline mixer, however, avoids the overlapping section by substituting the microstrip line with the slotline. This yields a shorter mixer chip which helps to reduce losses. Without the overlapping section, the fabrication process becomes easier to handle, and relaxes the computational requirements for a more accurate prediction of the design.

The profile of our unilateral finline taper is designed using the Optimum Taper Method for a minimum taper length at a required return loss, by tapering the cutoff frequency profile.[6] This ensures the high impedance of an unloaded waveguide to be transformed down smoothly without incurring high return loss. One unique advantage of a unilateral finline mixer is that the narrow slot at the end of the finline is a natural bandpass filter, avoiding unwanted IF signal leaking from the RF port to the IF port. The design has also been used previously with Transition Edge Sensors (TES) for C$_l$OVER project.[7]

Traditionally, finline mixers used thick quartz substrate (80–220 μm) to support the transmission line structure. Thick substrate occupies a substantial space within the waveguide and thus increase the dielectric loading loss. It also requires a deep groove in the waveguide wall for support. These grooves excite unwanted higher order modes in the waveguide and are especially detrimental to higher frequency applications.

In our new mixer design, the unilateral finline taper and all the superconducting circuitry is deposited on a 15 μm thin silicon substrate. This is made possible by the use of Silicon-On-Insulator (SOI) technology. The mixer chip is supported in the waveguide using gold beam leads positioned with the shallow locating pockets in the E-plane of the split mixer block. These gold beam leads are deposited on the substrate. They are only a few micron thick and thus the shallow groove has a negligible effect on the RF performance.

The mixer block design for the unilateral finline mixer chip is simple. It comprises a horn, a waveguide section, a pocket for the IF boards and pockets for the gold beam leads, all straightforward to fabricate.

Most of the submillimetre receiver arrays use corrugated horns to couple the RF signal from the sky to the mixer. Corrugated horns offer high aperture efficiency, high directivity, low sidelobes and low cross polarisation. To achieve this high performance, however, they require deep, high density grooves to be machined in the wall of the horn. This makes them expensive and time consuming to fabricate. A large fraction of the budget for constructing a multi-pixel receiver instrument is often attributed to the fabrication of high quality corrugated horns.

For our mixer design, we present a novel multi-flare angle smooth-walled horn design. These smooth-walled horns comprise a few discontinuities as shown in Figure 2. The position of the discontinuities and the magnitude of the flare-angles are determined by the required excitation of a combination of TE_{11}, TM_{11} and higher order modes to synthesise a uniformly polarised field distribution at the horn aperture. The satisfaction of this condition ensures a radiation pattern comparable to that of a corrugated horns.[8]

The advantages of smooth-walled horn over corrugated horn is therefore the ease of machining which reduces the cost and time of fabrication. This is because smooth-walled horns are made simply by drilling a profiled drill

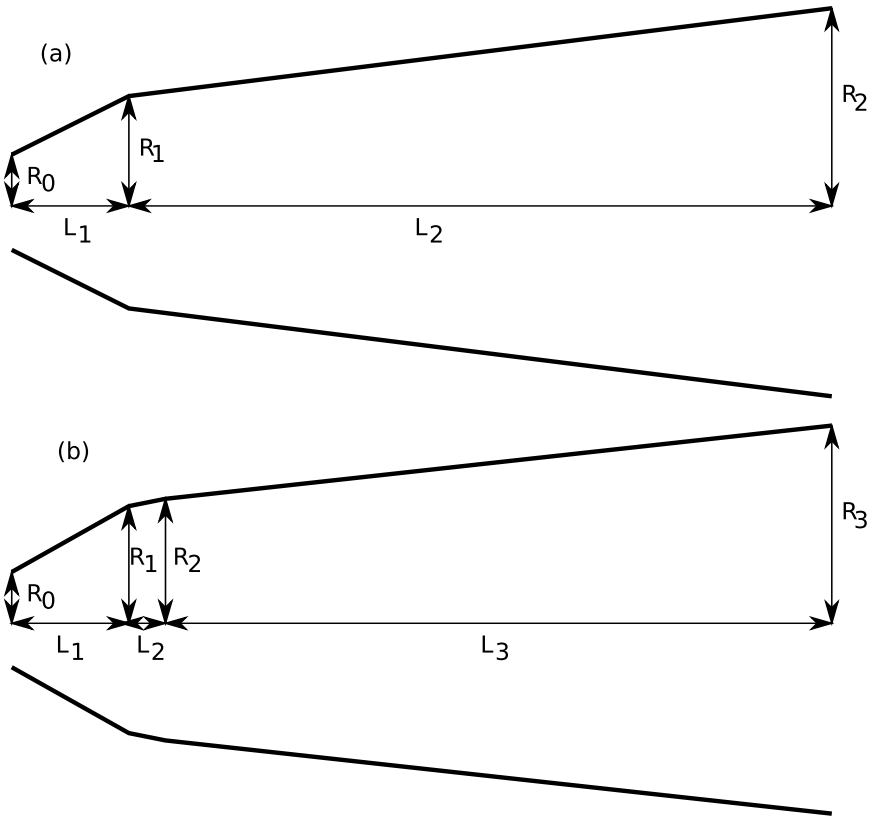

Figure 2. Schematic diagram showing (a) a 2-section smooth-walled horn with a discontinuity in flare angle and (b) a 3-section smooth-walled horn with two discontinuities in flare angle.

bit into an aluminium block via standard milling technique. Moreover, a whole feedhorn array may be fabricated by drilling individual horns into a single block of aluminium.

The above horn design has been studied extensively by Leech et. al.[9,10] at 230 GHz, both from designing and from manufacturing aspect. Their experimentally measured patterns agree well with the calculated beam patterns. In this paper, we report the result of our first attempt at designing and testing these direct-drilling smooth-walled horn at 700 GHz frequency band.

2. MIXER DESIGN

We present two designs of niobium based unilateral finline SIS mixers. The mixers are designed to operate from 600–700 GHz with 4–12 GHz IF bandwidth. The device is a 1 μm^2 circular Nb/AlO_x/Nb SIS tunnel junction with a normal resistance of approximately 20 Ω and a junction capacitance of 75 fF. Table 1 gives an overview of the material and the dimensions of various structures used in our design.

The mixer chip design is shown in Figure 3. It comprises 6 major sections: a 2-step matching notch, a unilateral finline taper, a finline-to-microstrip transition, a superconducting tuning circuit, an RF choke and an IF bonding pad. Most of these sections were designed using well known software packages such as Ansoft Designer and HFSS. The profile of the finline taper is determined using our own software package FinSynth,[6] to synthesise and analyse the taper using the Optimum Taper Method. To verify the final heterodyne performance, we use SuperMix,[11] an SIS mixer analysis package written by a research group at Caltech.

As shown in Figure 3, the major difference between the two layouts is in the way power is coupled from the finline to microstrip. The first design employs a direct slotline-to-microstrip transition (herein after known as the direct-mixer). The second design uses coplanar waveguide (CPW) sections with intermediate impedance to

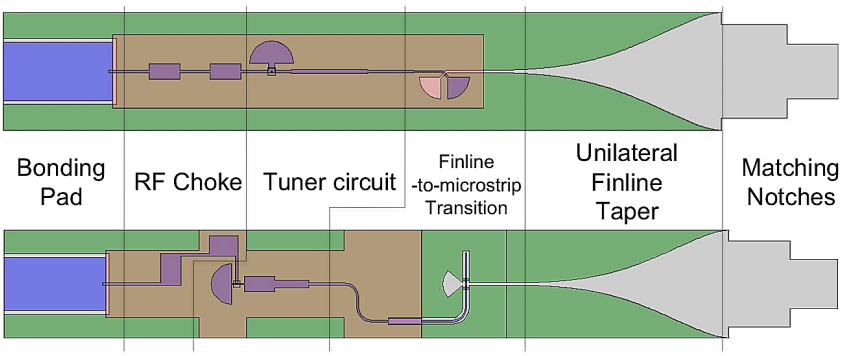

Figure 3. Overview of the unilateral finline mixer design, with two different types of finline-to-microstrip transition, showing the different components that make up the complete mixer chip.

Table 1. General material and dimension of our SIS mixer chips.

Structure	**Material**	**Dimension**
SIS junction	$Nb/AlO_x/Nb$	1 μm^2
Substrate	Silicon	15 μm
Ground plane	Niobium	250 nm
Dielectric layer	Silicon monoxide	475 nm
Signal layer	Niobium	400 nm
Waveguide	Aluminium	320×160 μm

match the higher impedance of the slotline to the lower impedance of the microstrip line (herein after known as CPW-mixer).

2.1 FINLINE-TO-MICROSTRIP TRANSITION

The impedance of the loaded waveguide is matched to the free space via a 2-step matching notch. These notches are about a quarter-wavelength long, and their widths are optimised to reduce return loss. The unilateral finline tapers down the impedance of the unloaded waveguide smoothly, and transforms the RF signal into a slotline mode. Since our SIS junction is fabricated across the microstrip line, which typically has a characteristic impedance close to the normal resistance of the junction (20 Ω), a transition from slotline to microstrip line is needed.

The transition from the high impedance slotline to microstrip line can be realised either through direct coupling of power across the dielectric layer, or more efficiently via intermediate CPW sections. In Figure 4 we show that both the slotline and the microstrip line are connected to a 90° radial stub approximately $\lambda_g/4$ in radius. At the crossing plane between the slotline and the microstrip, the slotline short-circuit radial stub appears as an open-circuit, and the microstrip open-circuit radial stub appears as a short-circuit. This combination guides the RF signal to propagate from the slotline to the microstrip line.

The advantage of the direct transition is that the different layers of material are clearly separated and the RF path can be arranged easily to align along the central axis to the chip. Its disadvantage is the restricted choice of appropriate characteristic impedance for dimensions that can be easily realised with photolithography. The narrowest slotline feasible with the available fabrication technology is about 2.5 μm, corresponding to about 70 Ω on a 15 μm silicon substrate. This is about 3 times higher than the characteristic impedance of a 2 μm microstrip line on the same substrate. One way to circumvent this problem is to include the impedance mismatch in the design of the transformer leading to the SIS junction. Another way is by using CPW as the intermediary type of transmission line to alleviate the mismatch, as we have done in our design.

CPW offers a wide range of impedance that can be easily manipulated to bridge the slotline-microstrip line mismatch. Its characteristic impedance is determined mainly by the ratio of the width of the central strip to

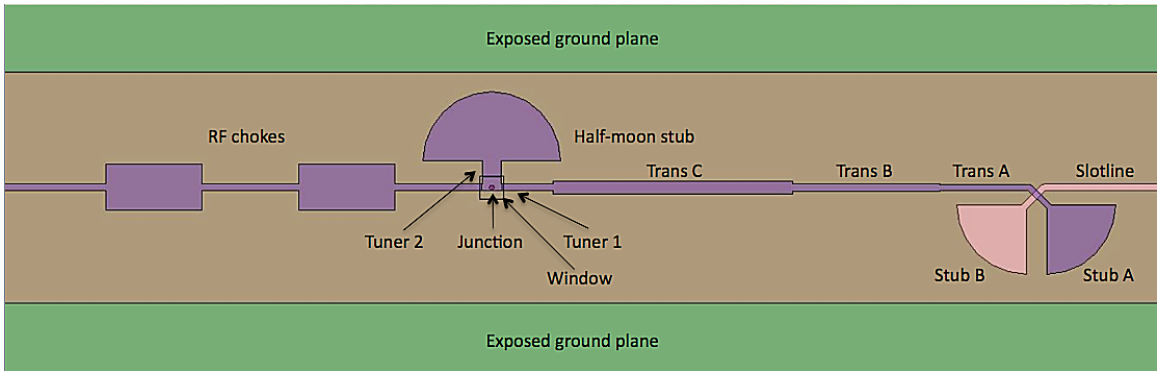

(a) Direct fineline-to-microstrip transition

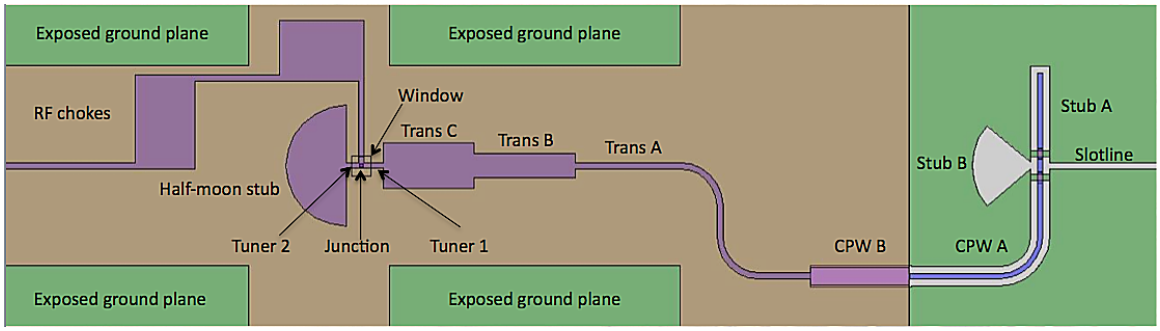

(b) Transition via coplanar waveguide

Figure 4. Two different types of unilateral finline SIS mixer employing SOI substrate. The "exposed ground plane" area is the region where the gold beamleads will be deposited. The oxide layer around the SIS junction, about 10μm wide, is deposited with only half the thickness of the dielectric layer. This ensure that the wiring layer had a good contact with the SIS junction.

the width of the gaps between the central strip and the ground plane. The RF power is guided from the slotline to the CPW using the same method as the direct transition. Here, the microstrip radial stub is replaced by a standard CPW stub. The two air-bridges near the crossing plane are placed to ensure the ground plane of the CPW have the same potential.

We would like to point out that the CPW-B section in Figure 4b is a modified CPW. The central strip and the ground plane are separated by the thin oxide layer. The gap is defined by the effective distance between the edge of the central strip on top of the oxide layer, and the edge of the ground plane beneath the oxide layer. This arrangement is made for two purposes. First, to bring the CPW central strip over the top of the oxide layer, preparing it to form a microstrip line. Second, it allows a very narrow CPW gap to be employed without worrying about shorting. This narrow gap is needed to achieve lower impedance without widening the central strip too much. Forming a microstrip line from this modified CPW section is straightforward: change the width of the central strip to the required microstrip width and close the ground plane channel of the CPW.

2.2 PLANAR CIRCUITRY

Our tuner circuit can be divided into 4 components: two inductive strips, a multi-section transformer and an RF choke. A lumped element model is shown in Figure 5 where the two inductive strips, one series to the junction, one parallel, are used to cancel out the junction capacitance at two slightly different frequencies. This provides two dips around the centre frequency in the matching diagram and thus helps to broaden the operating RF bandwidth.

The first inductor comprises a short microstrip section terminated with a half-moon stub that acts as a shorted load (refer to Figure 4). The radius of the half-moon stub is chosen to be about $\lambda_g/4$. The function of the short microstrip line is to transform the short-circuit stub into the inductance (seen by the junction) that

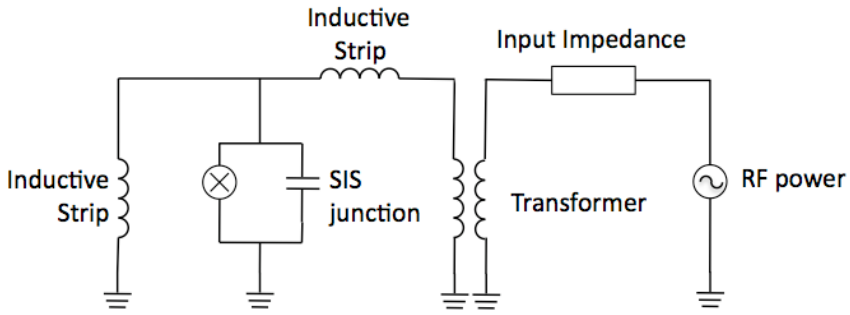

Figure 5. Electrical diagram of the RF tuning network for our finline mixers.

is required to counter-balance the junction capacitance, at a particular frequency. The width and the length of this microstrip line is calculated using

$$l = \frac{1}{Z_0 \beta \omega C}, \tag{1}$$

where $\beta = \frac{2\pi}{\lambda}$ is the wavenumber, ω is the radial frequency, C is the capacitance of the junction, Z_0 is the characteristic impedance of the microstrip line (corresponding to the width of the line), and l is the length of the microstrip line in the unit of electrical wavelength.

A single inductive strip is often used to tune out the junction capacitance, but this results in narrow band operation since the residual capacitance remains high at frequencies away from the tuned frequency. We thus place a second inductive microstrip line before the junction to tune out this residual capacitance at a slightly shifted frequency. The width and the length of this microstrip section can be determined using the standard transmission line equation,

$$Y_s = \frac{Y_l + iY_0 \tan \beta l}{Y_0 + iY_l \tan \beta l}, \tag{2}$$

where Y_s is the source impedance, Y_l is the load impedance (the residual impedance), Y_0 is the characteristic impedance of the line and βl is the propagation constant. By setting the imaginary part of Y_s to zero, the length of the microstrip line can be obtained in terms of βl. The value of Y_0 can be chosen to correspond to the desired width of the microstrip line.

To bridge the impedance difference of this sub-circuit (the SIS junction with two inductive strips) to the output of the finline-to-microstrip transition, a 3-step transformer is employed. It is worthwhile noting that the final design dimensions of this transformer and the two inductive microstrip lines are optimised using conventional 3-D electromagnetic simulation package such as HFSS to include the effects of superconducting surface impedance, dielectric thickness and tangential loss, and other factors.

An RF choke is normally placed after the SIS junction to avoid the RF signal leaking into the IF path. This ensure that most of the RF power is delivered to the junction. The choke consists of alternating high and low impedance $\lambda_g/4$ microstrip sections to provide high rejection ratio to the RF signal. The width of these sections are chosen to avoid the need for a wide microstrip line that can induce high IF capacitance.

All superconducting tuning circuitry, together with the finlines and finline-to-microstrip transition, are simulated in HFSS as one complete structure. This helps to understand the electromagnetic behaviour of the complete mixer chip, taking into account the effect of all the interfaces involved. Figure 6 shows the return loss and the insertion loss of the complete RF design predicted by HFSS. Both direct-mixer and CPW-mixer design yield about 100 GHz operating RF bandwidth centred at 650 GHz. The power coupled to the junction is better than –0.5 dB in both cases, within the design bandwidth.

The physical structure of the on-chip superconducting circuitry including the SIS junction and the finline taper will be seen as a lumped RLC load at IF. To ensure our mixers have a wide IF bandwidth, matching that of the IF gain chain, we use a transformer to match this RLC load to the 50 Ω input impedance of the

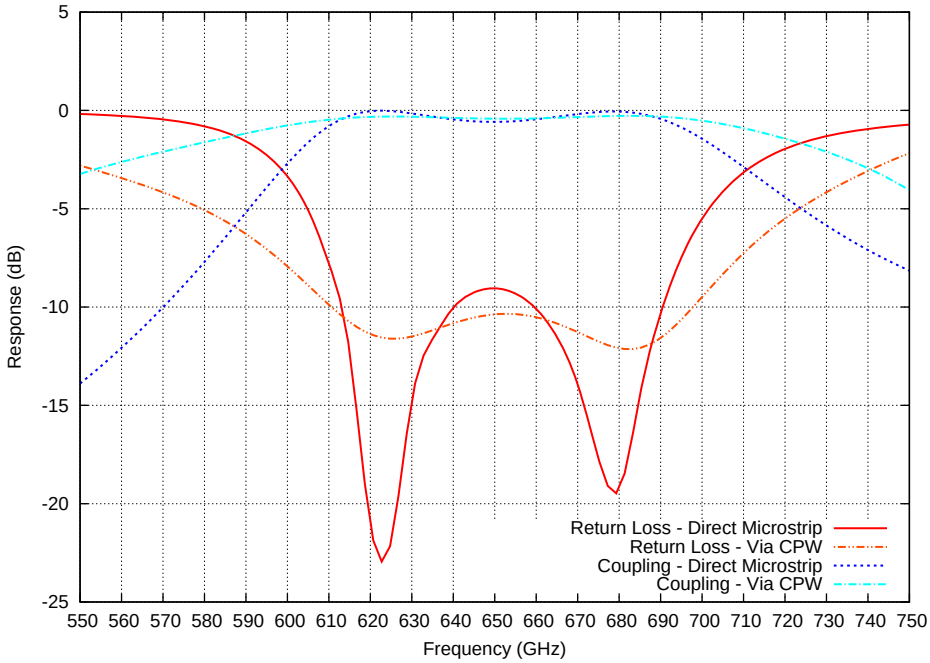

Figure 6. HFSS simulation shows that the tuner design exhibit broad bandwidth, with about 100 GHz centred at 650 GHz.

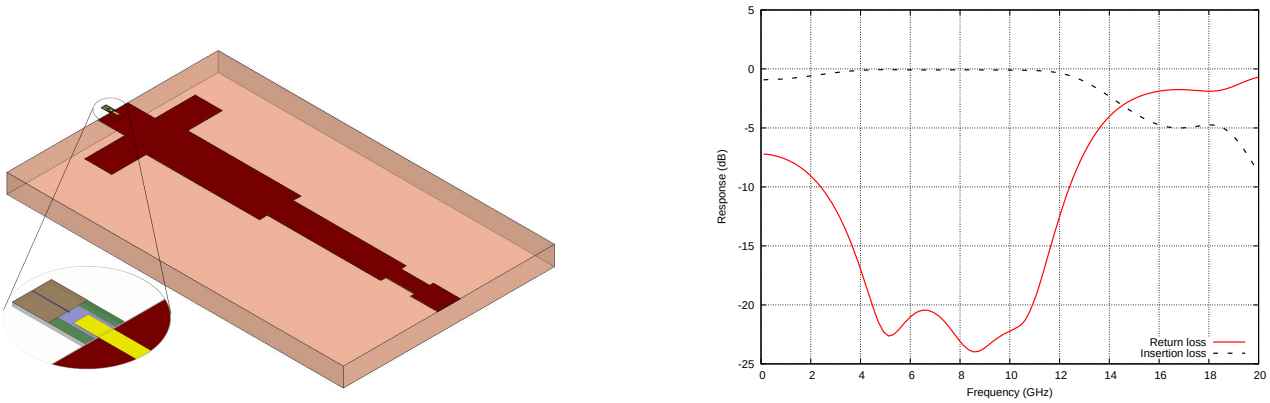

(a) Diagram of IF transformer. (b) Insertion and return loss

Figure 7. IF transformer to match the output complex impedance of the mixer chip to the 50 Ω IF output. HFSS simulation shows that the transformer had better than -15 dB return loss from 4 GHz to 12 GHz IF band.

low-noise amplifier (LNA). We use HFSS to design the IF transformer to make certain we include the effect of the inductance induced by structure such as the bonding pad and the gold beam leads. As can be seen in Figure 7, this results in a 5-step transformer and it has a very flat insertion loss over ∼8 GHz from 4–12 GHz. This matches well with the operating bandwidth of our LNA, and is wide enough for most astronomical requirements.

2.3 SIMULATION RESULTS

For analysing the behaviour of our mixers, we use both HFSS and SuperMix. HFSS can provide accurate description of the electromagnetism behaviour and SuperMix has the ability to simulate the superconducting mixer performance. We include the superconducting surface impedance effect in all the components simulated in HFSS. The scattering matrices of all these components are then exported to SuperMix to form the SuperMix mixer circuit shown in Figure 8.

In Figure 9, we show the calculation results of both mixer designs described previously. All these results were

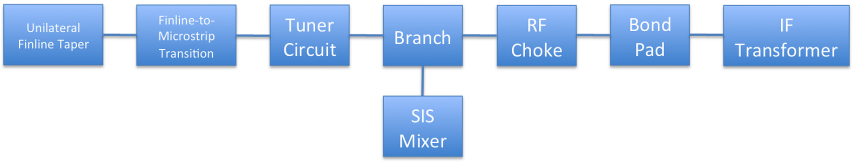

Figure 8. Block diagram shows the various components included in the SuperMix simulation.

simulated using an IV curve obtained experimentally from an antipodal-finline-tapered 700 GHz balanced SIS mixer fabricated previously.[12] Noted that this was our first attempt at testing this antipodal balanced SIS mixer at 700 GHz, thus the obtained IV curve does not represent its best performance. Consequently, the simulated results from SuperMix for our new mixer designs might be slightly degraded. Figure 9a and Figure 9b show that the noise temperature predicted is below 70 K across the operating RF bandwidth. This, however, can be halved, by using an ideal IV curve.

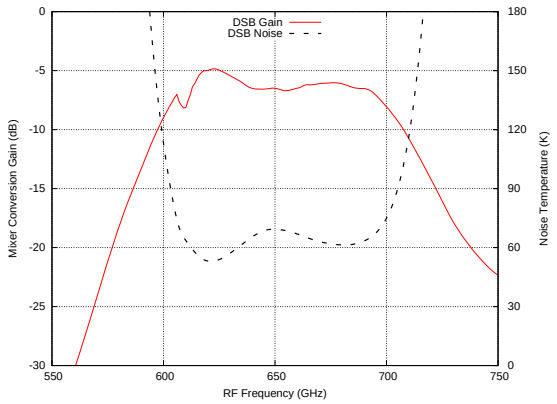

(a) RF response of direct-mixer

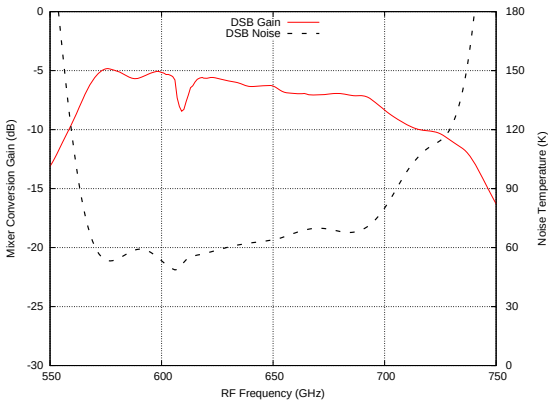

(b) RF response of cpw-mixer

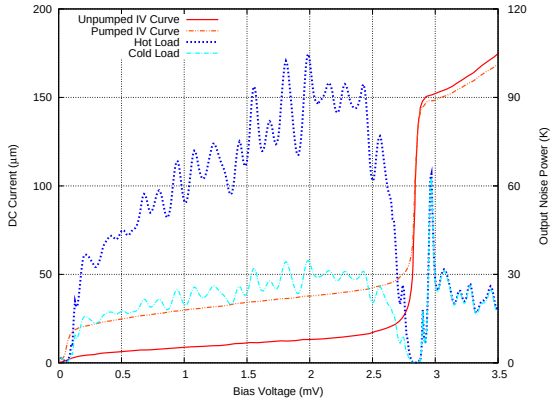

(c) IV curves and IF output power

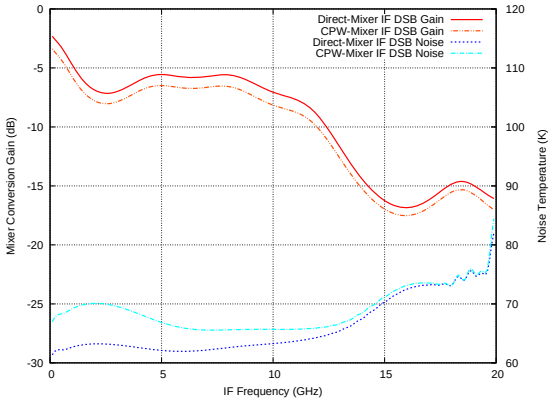

(d) IF gain

Figure 9. SuperMix simulation shows the results of heterodyne performance of the direct-mixer and cpw-mixer chip. The unpumped IV curve used as an input to SuperMix is a measured IV curve of a balanced antipodal finline mixer fabricated previously for operating in 700 GHz band. All the response curves are generated using the following setting: biased at 2.2 mV, pumped at 670 GHz with LO power of 100 nW and IF frequency set at 1.5 GHz. Curves in sub-figure 9c is generated using the direct-mixer design.

The above analysis using the measured IV curve indicates that the new mixer design has excellent performance across a wide RF band. The RF gain is flat and the noise temperature is stable across the band. The CPW-mixer has a slightly wider bandwidth due to the better impedance matching of the slotline to the microstrip line as

discussed in Section 2.1. With the IF transformer installed, the roll-off of the IF gain is also flat across the desired IF bandwidth. The noise temperature is smooth from 4–12 GHz at about 65 K.

3. FEEDHORN

Our mixer block employs a 3 flare-angled horn. Since the output of the feedhorn is a circular waveguide, a transition from circular to rectangular waveguide is required. To realise this transition, we drill a 10° semi-flare angle opening cone into the inlet of the rectangular waveguide, as shown in Figure 10. The depth of the drilling is determined by the diameter required to match that of the circular waveguide. This simple method of making a transition is examined using HFSS and the simulated return loss across the operating band is less than –20 dB.

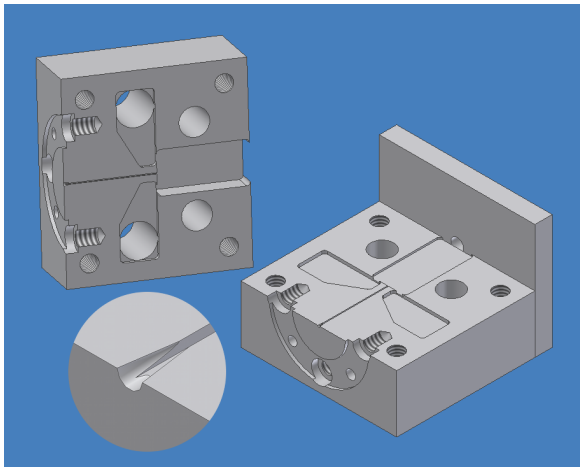

(a) Mixer block

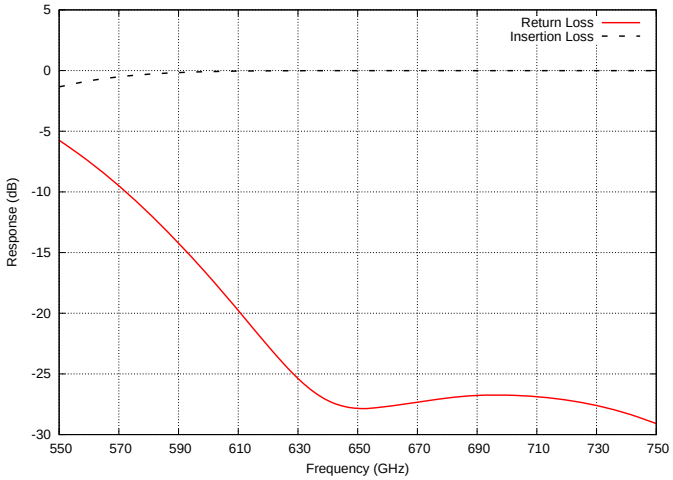

(b) Insertion and return loss

Figure 10. The drawing of the split-block that will be used to house the mixer chip. The two butterfly-wing-structure are used to hold the iron plate that couples the magnetic field from the coil to suppress the Josephson current. It will be fed from the two poles on top of the mixer block. The IF output will be tapped from the IF board using standard SMA connector at the back of the mixer block. The IF board is placed in the pocket immediately after the rectangular waveguide. Return loss and insertion loss for the circular to rectangular waveguide with an opening angle of 10° is less than –20 dB over the operating bandwidth. The input throat opening of the smooth-walled horn is 408 μm. The 10° opening cone is drilled only after the rectangular waveguide is milled within the split-block.

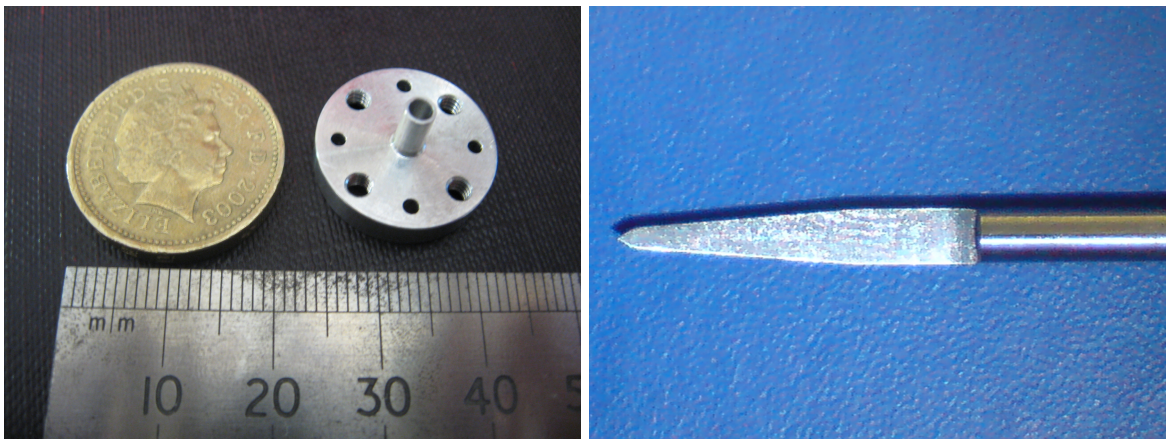

Figure 11. The 700 GHz smooth-walled horn that is used to feed the RF signal to the mixer chip. The drill bit is made of high-speed steel produced with the cutting edge shaped to the required feedhorn profile.

In order to investigate the suitability of using these smooth-walled horns at the RF frequency band of our finline mixers, we fabricated a few 3 flare-angled horns of this type using the direct-drilling method. The actual horn and the drilling tool used is shown in Figure 11. The tolerance required to achieve good performance at this frequency is stringent. For measuring the far field beam patterns of these horns, we also fabricated the 10° opening cone circular-to-rectangular waveguide transition describe above as a separate piece to fit the flange of our local oscillator (LO).

We measured the far field radiation patterns of the smooth-walled horn using a custom far field test facility equipped with a 4 K cryogenic bolometric detector. The feedhorn under test is aligned and fastened to the circular-to-rectangular waveguide transition, which in turn is affixed to the LO source. This entire arrangement is then rotated using a motorised rotary table with the rotating axis aligned with the horn aperture. We placed some Eccosorb RF absorber at the key positions around the experimental setup to eliminate stray power pickup by the horn under test and to reduce the effect of standing waves. The separation distance between the horn under test and the window of the cryogenic dewar housing the detector is about 378 mm. This distance is sufficient to ensure that we are in the far field region ($10D^2/\lambda = 33.6$mm).

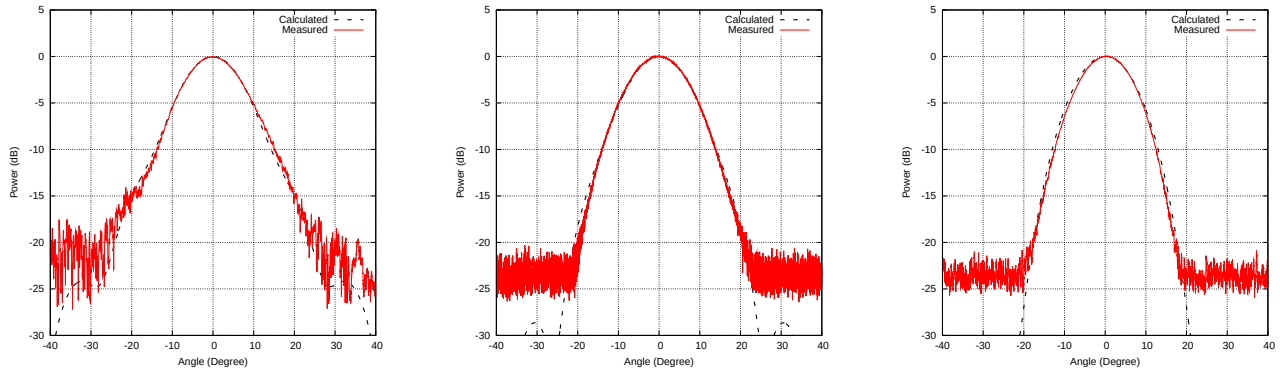

(a) 600 GHz E-Plane (b) 650 GHz E-Plane (c) 700 GHz E-Plane

(d) 600 GHz H-Plane (e) 650 GHz H-Plane (f) 700 GHz H-Plane

Figure 12. Beam pattern measurements of the 700 GHz smooth-walled horn across the 650 GHz frequency band at E- and H-plane. The measured beam pattern match very well, given the tight tolerances of standard drilling and milling techniques at this wavelength.

Figure 12 shows the comparison of the measured far field beam patterns with the theoretical predictions obtained using the modal matching method. The results represent our first attempt to measure the far field radiation patterns of this smooth-walled horn design at 700 GHz frequency band. It can be seen that the main beams measured from 600 GHz to 700 GHz are almost identical to the theoretically predicted far field patterns. No obvious sidelobe is detected within the dynamic range as expected. The main beams are smooth, symmetric

and clear of standing wave ripples. This indicates that the simple direct-drilling method for producing low-cost high-quality feedhorn is feasible even at frequencies as high as 700 GHz.

4. CONCLUSION

We have presented the design of two broadband unilateral finline SIS mixers at 650 GHz. The novel features in this design are the employment of unilateral finline taper, thin silicon substrate using SOI technology, and a multi-flare angle smooth-walled horn replacing the conventional corrugated feedhorn. The use of unilateral finline taper yields a shorter and easier to fabricate mixer chip while retaining a wide substrate area for elegant integration of superconducting circuitry. Thin silicon substrate ensures that the lightweight mixer chip can be held within the waveguide without the need of deep grooves in the waveguide wall, avoiding the excitation of unwanted higher order modes. Both designs result in a tunerless and easy to fabricate mixer block. We have modelled the electromagnetic and detector behaviours of the whole mixer chip rigorously by feeding the S-parameters of the passive superconducting chip into SuperMix. Using an experimental IV curve, we find that the RF noise temperatures are low and flat over a wide range of frequencies. The RF gain is also flat across a 100 GHz bandwidth. The IF performance is satisfactory from 4–12 GHz, matching well with the operating bandwidth of our IF chain. Finally, we demonstrate that the multi-flare angle smooth-walled horn fabricated using the novel direct-drilling technique can yield quality performance at the 700 GHz band. The measured beam circularity at various frequencies are good, and the sidelobes are low. Above –20 dB level, the far field beam patterns measured agree well with the theoretical predictions.

ACKNOWLEDGMENTS

This project is partially funded by AMSTAR+ of RadioNet and an STFC follow-on-fund grant.

REFERENCES

[1] Groppi, C., Walker, C., Kulesa, C., Golish, D., Kloosterman, J., Weinreb, S., Jones, G., Barden, J., Mani, H., Kuiper, T., Kooi, J., Lichtenberger, A., Cecil, T., Narayanan, G., Pütz, P., and Hedden, A., "SuperCam: A 64 Pixel Heterodyne Array Receiver for the 350 GHz Atmospheric Window," in [*Proceedings of the twentieth International Symposium on Space Terahertz Technology, held April 20-22, 2009, in Charlottesville, VA, USA. Edited by Eric Bryerton, Anthony Kerr, and Arthur Lichtenberger. Sponsored by National Radio Astronomy Observatory (NRAO), the University of Virginia (UVA), and Virginia Diodes, Inc. (VDI). 2009, p.90*], E. Bryerton, A. Kerr, & A. Lichtenberger, ed., 90–+ (Apr. 2009).

[2] Robson, I. and Holland, W., "SCUBA-2: The Submillimeter Mapping Machine," in [*From Z-Machines to ALMA: (Sub)Millimeter Spectroscopy of Galaxies*], A. J. Baker, J. Glenn, A. I. Harris, J. G. Mangum, & M. S. Yun , ed., *Astronomical Society of the Pacific Conference Series* **375**, 275–+ (Oct. 2007).

[3] Yassin, G., Padman, R., Withington, S., Jacobs, K., and Wulff, S., "Broadband 230 GHz finline mixer for astronomical imaging arrays.," *Electronics Letters* **33**, 498–500 (Mar. 1997).

[4] Yassin, G., Withington, S., Buffey, M., Jacobs, K., and Wulff, S., "A 350-GHz SIS antipodal finline mixer," *IEEE Transactions on Microwave Theory Techniques* **48**, 662–669 (Apr. 2000).

[5] P., K., A., J., G., Y., S., W., and J., L., "The design of Potter horns for THz applications using a genetic algorithm," *Int. J. Infrared Milli. Waves* **28**, 1103–1114 (2007).

[6] North, C., Yassin, G., and Grimes, P., "Rigorous Analysis and Design of Finline Tapers for High Performance Millimetre and Submillimetre Detectors," in [*Seventeenth International Symposium on Space Terahertz Technology, held May 10-12, 2006 at Observatoire de Paris, LERMA. Paris, France., p.284-287*], A. Hedden, M. Reese, D. Santavicca, L. Frunzio, D. Prober, P. Piitz, C. Groppi, & C. Walker, ed., 284–287 (May 2006).

[7] Audley, M. D., Barker, R. W., Crane, M., Dace, R., Glowacka, D., Goldie, D. J., Lasenby, A. N., Stevenson, H. M., Tsaneva, V., Withington, S., Grimes, P., Johnson, B., Yassin, G., Piccirillo, L., Pisano, G., Duncan, W. D., Hilton, G. C., Irwin, K. D., Reintsema, C. D., and Halpern, M., "TES imaging array technology for C_lOVER," in [*Society of Photo-Optical Instrumentation Engineers (SPIE) Conference Series*], *Society of Photo-Optical Instrumentation Engineers (SPIE) Conference Series* **6275** (July 2006).

[8] Yassin, G., Kittara, P., Jiralucksanawong, A., Wangsuya, S., Leech, J., and Jones, M., "A High Performance Horn for Large Format Focal Plane Arrays," in [*Proceedings of the Eighteenth International Symposium on Space Terahertz Technology, held March 21-23, 2007, at California Institute of Technology, Pasadena, CA USA. Edited by Alexandre Karpov. 2007, p.199*], A. Karpov, ed., 199–+ (2007).

[9] Kittara, P., Leech, J., Yassin, G., Tan, B. K., Jiralucksanawong, A., and Wangsuya, S., "High performance smooth-walled feed horns for focal plane arrays," in [*Proceedings of the Ninteenth International Symposium on Space Terahertz Technology, held April 28-30, 2008, in Groningen. Edited by Wolfgang Wild. Sponsored by SRON, Netherlands Institute for Space Research, TUDelft, Delft University of Technology, and the University of Groningen. 2008, p.346*], W. Wild, ed., 346–+ (Apr. 2008).

[10] Leech, J., Yassin, G., Tan, B. K., Tacon, M., Kittara, P., Jiralucksanawong, A., and Wangsuya, S., "A New, Simple Method for Fabricating High Performance Sub-mm Focal Plane Arrays by Direct Machining using Shaped Drill Bits," in [*Proceedings of the 20th International Symposium on Space Terahertz Technology, held April 20-22, 2009, in Charlottesville, VA, USA. Edited by Eric Bryerton, Anthony Kerr, and Arthur Lichtenberger. Sponsored by National Radio Astronomy Observatory (NRAO), the University of Virginia (UVA), and Virginia Diodes, Inc. (VDI). 2009, p.214*], E. Bryerton, A. Kerr, & A. Lichtenberger, ed., 214–+ (Apr. 2009).

[11] Ward, J., Rice, F., Chattopadhyay, G., and Zmuidzinas, J., "SuperMix: A Flexible Software Library for High-Frequency Circuit Simulation, Including SIS Mixers And Superconducting Elements," in [*Proceedings of the Tenth International Symposium on Space Terahertz Technology, held March 16-18, 1999, at the University of Virginia, Charlottesville, VA USA. Organized by University of Virginia, Applied Electrophysics Laboratory. Organizing committee: Thomas W. Crowe and Robert M. Weikle. 1999, p.268*], T. W. Crowe & R. M. Weikle, ed., 268–+ (Mar. 1999).

[12] Grimes, P., Yassin, G., Jacobs, K., and Withington, S., "A 700 GHz single chip balanced SIS mixer," in [*Sixteenth International Symposium on Space Terahertz Technology, held May 2-4, 2005 at Chalmers University of Technology. Göteborg, Sweden., p.46-52*], 46–52 (May 2005).